

Dynamics of folding in Semiflexible filaments

P. Ranjith * and P.B. Sunil Kumar[†]

Department of Physics, Indian Institute of Technology, Madras

Chennai 600 036,

India

(November 1, 2018)

Abstract

We investigate the dynamics of a single semiflexible filament, under the action of a compressing force, using numerical simulations and scaling arguments. The force is applied along the end to end vector at one extremity of the filament, while the other end is held fixed. We find that, unlike in elastic rods the filament folds asymmetrically with a folding length which depends only on the bending stiffness κ and the applied force f . It is shown that this behavior can be attributed to the exponentially falling tension profile in the filament. While the folding time τ_0 depends on the initial configuration, the distance moved by the terminal point of the filament and the length of the fold scales as $\tau^{1/2}$ at time $\tau \gg \tau_0$ and is independent of the initial configuration.

PACS : 82.35.Lr, 87.15.-v, 87.15.Aa, 87.80.Cc

Typeset using REVTeX

*Email:ranjith@physics.iitm.ac.in

[†]Email:sunil@physics.iitm.ac.in

Recent developments in micro manipulation techniques using optical tweezers, micro pipette and high resolution optical imaging have made the study of single filament dynamics experimentally feasible [1–3]. Today it is possible to apply forces of the order of pico Newton with precision. This has spurred lot of activity in the study of single bio-polymers. These techniques have been used extensively in the study of stretching elasticity and force extension relation of bio-polymers [1,4,5]. Some of these techniques can also be applied to study the effect of compressing forces on single polymer filaments [4,5].

In a physical description of their statistical properties, the chemical details of polymers can be summarized using a set of parameters. These parameters characterize the individual features of each polymer species. Two of the most important parameters are persistence length and bending stiffness. Persistence length, l_p , is the distance along the contour of the filament over which the tangent-tangent correlation is destroyed by thermal fluctuations. Semiflexible polymers have contour length comparable to its persistence length. This means that unlike in the case of flexible filaments or rigid rods the dynamical properties of semiflexible filaments are determined by both conformational entropy and bending stiffness. Thermal fluctuations also play an important role in determining the viscoelastic behavior of semidilute solutions of semiflexible filaments [6,7].

From the biological point of view, a study of the mechanical and statistical mechanical properties of semiflexible filaments are important to understand the dynamical behavior of cytoskeletal network. Cytoskeleton, which controls the shape recovery and dynamic cellular reorganization of living cells is a complex network of polymers [8]. At the length scale of a cell most of the polymers which build up this network are semiflexible [9]. Microtubules, $l_p = 5.2mm$ [10], and Actin filaments, $l_p = 17\mu m$ [11] are some of the examples.

For length scales much smaller than the persistence length the filaments are like rigid rods. Under the action of longitudinal compressing forces these filaments exhibit the classical Euler buckling [12]. The dynamics of this buckling has been studied recently [13]. In the case of bio-polymers like microtubules, such buckling is also observed as a result of the force generated by polymerization [3] and by the movement, on them, of kinesin motors

[14]. On the other hand in flexible polymers with persistence length much smaller than the contour length, the compression forces applied at the extremities do not propagate along the polymer. This naturally raises the question, what happens when we apply a longitudinal compressing force on a semiflexible filament? Here we investigate the dynamics of a single semiflexible filament under the action of an external compressing force.

In this paper we look at the folding of a semiflexible filament under the action of a compressing force acting along the end to end vector. Previous calculations of folding in semiflexible polymers assumes uniform tension in the filament [15,13]. We show that, at finite temperature, the tension profile in a semiflexible filament in equilibrium decreases exponentially along the contour. This tension profile is shown to have non trivial effects on the folding dynamics of filaments. The filament is described by the position vector $\mathbf{r}(s)$, parameterized by the contour length s of the filament, where $0 \leq s \leq L$. Variety of boundary conditions are possible. Throughout this paper we will discuss only the case wherein the curvature of the filament at the two extreme ends are zero (hinged boundary). This implies free rotation of the tangent vector at the ends. The $s = 0$ tip of the filament is allowed to move only along the direction of the end to end vector which is taken to be along the x -axis. The position of the $s = L$ tip, $\mathbf{r}(L)$, is fixed. An external force \mathbf{f} is applied at the $s = 0$ tip along the x -direction. A detailed discussion of other possible boundary conditions will be published elsewhere [16]. The elastic coefficients for the transverse and longitudinal fluctuations of semiflexible filaments are not the same. This implies that, for the above boundary conditions, a compressing force could lead to either folding or buckling. However, the transverse spring coefficient in the stiff limit is proportional to stiffness κ and the longitudinal spring coefficient proportional to κ^2/T [17]. Thus an applied force on a filament with hinged ends will always lead to folding.

Actin filaments exhibit a persistence length of about $17\mu m$ at room temperature [11]. Critical force for buckling is then of the order of a few pico Newton. In a laser tweezers experiment we can apply forces of the order of pico Newton with precision. Typically, in such experiments the filament is held by a bead of size $\sim 0.5\mu m$ to a precision of $\sim \pm 50nm$

[18]. In view of these, it should be possible to observe folding dynamics in laser tweezers experiments using actin filaments of length $< 10\mu m$ or microtubules of length $> 100\mu m$.

In our numerical simulations, semiflexible filament are modeled as N rods of equal length hinged together linearly. Position of each hinge is defined by the Cartesian coordinates $\mathbf{r}_i = (x_i, y_i)$. The total energy of the filament, with the compressing force \mathbf{f} acting at \mathbf{r}_1 , is [19],

$$F = \frac{\kappa}{2} \sum_{i=1}^{N-2} (1 - \mathbf{t}_i \cdot \mathbf{t}_{i+1}) + \sum_{i=1}^{N-1} g_i \mathbf{t}_i^2 - x_1 \hat{\mathbf{e}}_x \cdot \mathbf{f}, \quad (1)$$

where \mathbf{t}_i is the unit vector pointing from i to $i + 1$. The first term is the contribution from the curvature of the polymer, κ being the elastic constant, and the second term is to enforce the local inextensibility condition, $\mathbf{t}_i^2 = 1$, of the rods. We work in the over damped limit where the dynamics of the filament is described by the Langevin equations:

$$\begin{aligned} \Gamma^{-1} \frac{\partial x_i}{\partial t} &= -\frac{\partial F}{\partial x_i} + \eta_{x_i}(t) \\ \Gamma^{-1} \frac{\partial y_i}{\partial t} &= -\frac{\partial F}{\partial y_i} + \eta_{y_i}(t). \end{aligned} \quad (2)$$

Here the effect of the solvent enters only through the inverse friction coefficient Γ . Equations 2 are solved along with the constraint $\mathbf{t}_i^2 = 1$. The noise η obeys the fluctuation dissipation theorem which in the case of filaments with equal monomer mass leads to [20]

$$\langle \eta_{x_i}(t) \eta_{y_j}(t') \rangle = 2\Gamma^{-1} \delta_{xy} \delta_{ij} \delta(t - t').$$

Integrating equations 2 we get the increments Δx_i and Δy_i , which are functions of the unknown Lagrange multipliers g_i . Increment in time is represented by the dimensionless variable $\Delta\tau = \Gamma\Delta t$. The coordinates of the vertices at time $\tau + \Delta\tau$ obtained from the above equations have to satisfy the constraint $\mathbf{t}_i^2(\tau + \Delta\tau) = 1$. These $N - 1$ simultaneous nonlinear equations are solved to determine the Lagrange multipliers g_i . We choose $\Delta x_N = 0$, $\Delta y_N = 0$ and $\Delta y_0 = 0$ at all times. There is no constraint on the angle between the filament and the force direction at both ends.

We have carried out extensive numerical simulation of the above model using a chain with length $N = 150$ for different values of κ and f . One run in the simulation correspond to $\Delta\tau = 1$. All results are averaged over 10 initial configurations. The initial conformation of the filament ($\tau = 0$) is chosen from an equilibrium distribution which satisfy the boundary condition $y_1 = 0$ and $y_N = 0$ [22]. The snapshots from our simulation for a constant applied force f is shown in figure 1. We observe that the filament first develop a fold at a distance l_f from the end at which the force is applied. l_f is the position of the first maximum in curvature along the contour when the free end is perpendicular to the end to end vector. For a given κ and force f , this "folding length" (l_f) is independent of the initial configuration and is found to depend on bending stiffness as $l_f \sim \sqrt{\kappa}$. This is shown in figure 2.

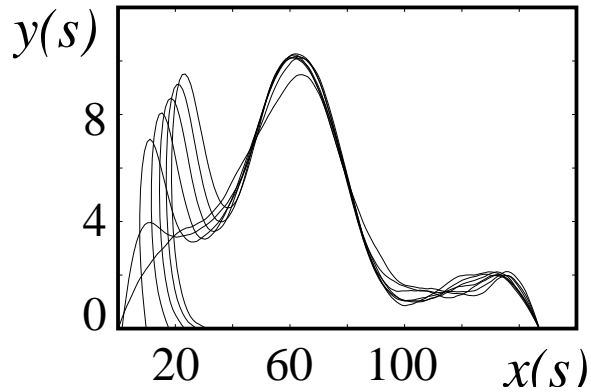


FIG. 1 The snapshots of conformations of a semiflexible filament with $\kappa = 500$ and $N = 150$, taken at equal intervals of time $\Delta\tau = 0.2$ million for an applied force $f = 30$.

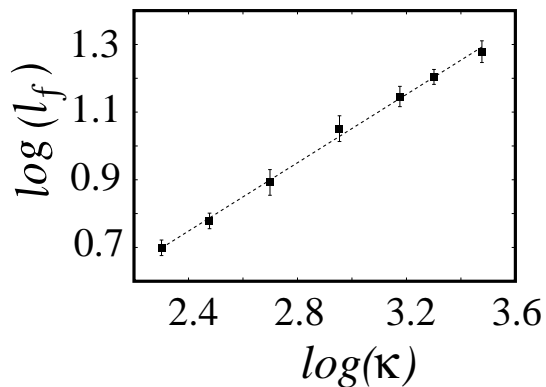


FIG.2 A plot of $\log_{10} \kappa$ vs $\log_{10} l_f$. The filled squares are from the simulation. The dotted line is a fit which shows $l_f \sim \sqrt{\kappa}$.

A better understanding of the dependence of folding length on κ is obtained from the continuum equations for the worm like chain model [21,22]. The equation of motion in the over damped limit for the boundary conditions, $\mathbf{r}(L) = \text{a constant}$ and $y(0) = 0$, is then

$$\begin{aligned} \frac{1}{\Gamma} \frac{\partial \mathbf{r}}{\partial t} = -\frac{\delta F}{\delta \mathbf{r}} = & -l_p \partial_s^4 \mathbf{r} + 2\partial_s(g\dot{\mathbf{r}}) \\ & + \left(f + 2g(s)\dot{\mathbf{r}}(s) - l_p \partial_s^3 \mathbf{r} \right) \delta(s) + \eta(s, t), \end{aligned} \quad (3)$$

here dots denote the derivatives with respect to arc length. $\eta(s, t)$ is the thermal noise and Γ is a kinetic coefficient. Using the constraint $\dot{\mathbf{r}}(s)^2 = 1$, and equation 3 we get,

$$\frac{1}{2\Gamma} \frac{\partial \dot{\mathbf{r}}^2}{\partial t} = 2\ddot{g} - 2g\ddot{r}^2 - l_p \dot{\mathbf{r}} \cdot \partial_s^5 \mathbf{r} = 0. \quad (4)$$

Comparing the curvature and force terms in equation 3, we get a length which scales as $l \sim \sqrt{(\kappa/f)}$. Similar length scale is also obtained from the constraint equation.

Let us try to get some insight into the tension profile along the filament. Dropping higher order derivative terms from the constraint equation 4 leads to

$$\frac{1}{2\Gamma} \frac{\partial \dot{\mathbf{r}}^2}{\partial t} = \ddot{g}^f - g^f \ddot{r}^2 = 0. \quad (5)$$

We use g^f to distinguish this tension from that obtained with κ . Numerical solution of the above equation for time $t = 0$ is shown in figure 3. Here we have replaced $\ddot{\mathbf{r}}(s)^2$ by its approximate ensemble averaged value

$$\langle \ddot{r}(s)^2 \rangle = \left(\frac{1}{l_p L} \right) \frac{\sum_n \sin^2 \left(\frac{n\pi s}{L} \right)}{1 - \frac{L}{\kappa\pi} \sum_n \frac{1}{n^2} \sin^2 \left(\frac{n\pi s}{L} \right)} \quad (6)$$

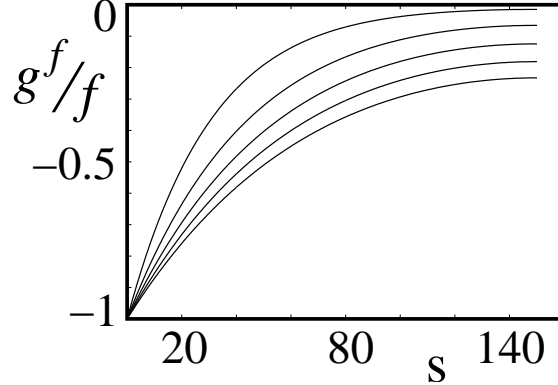


FIG.3 $g(s)$ obtained from equation 5 for $\kappa = 500, 1000, 1500, 2000, 2500$ and $n=150$.

We see that the resulting tension decays exponentially. We find the length scale to vary as $\sqrt{\kappa}$. The tension profile is found to depend on the number of modes taken in equation 6 and is exponential only in the limit when the number of modes are large. The lower cut off in length being set by the segment length.

We now compare this tension profile with that obtained from the simulations. In the simulations, the tension g_i has contributions from three sources, namely, curvature, noise and the applied force. Like in the case of continuum equations we can calculate a tension g_i^f by setting the noise and curvature terms to zero. Since the equations of motion are nonlinear one may doubt the validity of a comparison between the tension g_i^f obtained from this calculation with $g^f(s)$ obtained from the continuum equations. To dispel this doubt we linearize the equations for the tension profile by neglecting terms of the order $(\Delta x_i)^2$ and $(\Delta y_i)^2$, in equation $\mathbf{t}_i^2 = 1$. The results obtained from such a linear calculation agree well with the full non-linear results (data not shown). However, this linearization also means deviation from the constraint $\mathbf{t}_i^2 = 1$. Even for small $\Delta\tau$ these errors in segment length can become very large in a short time. Therefore we have to use the full non-linear equations for updating the filament configuration.

In figure 4 we show this tension profile g_i^f as a function of the vertex index i . The tension g_i^f goes to zero exponentially as predicted earlier. The distance ξ over which the tension falls to half its maximum value is found to increase as $\sqrt{\kappa}$ for a fixed value of f .

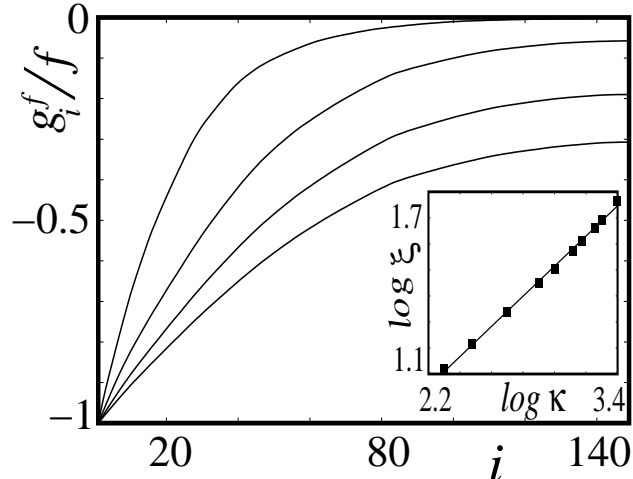


FIG.4 g_i^f/f as a function of the contour length i from the point at which force is applied, for $\kappa = 300, 1000, 2000, 3000$. Inset: $\log(\kappa)$ is plotted against the $\log \xi$, showing $\xi \sim \kappa^{1/2}$

We now look at how the buckling length l_f depends on the applied force f . We have seen in the previous paragraph that the tension in a semiflexible filament falls exponentially along its contour. This exponential tension profile differentiates between semiflexible filaments and stiff elastic rods wherein the tension profile is uniform. Thus it is instructive to extend the stability calculations for a rod with uniform tension [12] to the present case of exponential tension profile of the form $\exp(-\alpha s/\sqrt{\kappa}) + 1$. The equation of equilibrium is,

$$\kappa \frac{\partial^4 y}{\partial s^4} + \frac{f}{2} \frac{\partial}{\partial s} \left[\frac{\partial y}{\partial s} \left[\exp(-\alpha s/\sqrt{\kappa}) + 1 \right] \right] = 0. \quad (7)$$

These equations are solved numerically with the boundary conditions $\ddot{y}|_{s=L} = 0$, $\ddot{y}|_{s=0} = 0$, $y(0) = 0$, $y(L) = 0$. The lowest energy solutions of this equation show that the value $s = s_{max}$, of the first maximum in curvature, shifts to smaller values of s with increasing f . This is indeed what we see in our simulations of the semiflexible filament.

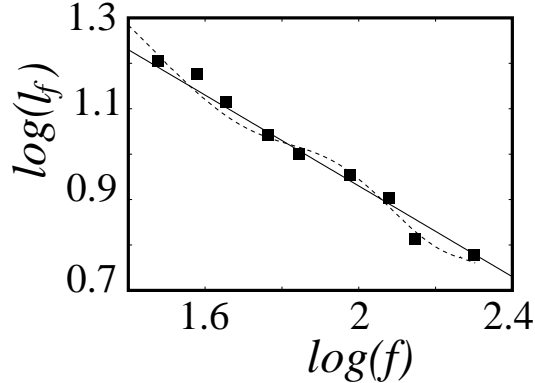


FIG.5 Folding length (l_f) as a function of the applied force(f); The dotted line represents the buckling point obtained from the numerical solution of equation 7 with $\alpha = 10$. The straight line corresponds to $l_f \sim \frac{1}{\sqrt{f}}$

In figure 5 we compare the buckling length l_f obtained from the simulation with s_{max} from the solution of equation 7. α is the only adjustable parameter used to get the agreement between the two results.

We now come to the dynamical behavior of the fold. The length of the segment before the fold, the end to end distance and tension g_i^f all depend on time. As can be seen from the configuration snap shots in figure 1, once the filament has folded the applied force acts to *pull* the filament. This implies a change in sign of tension g_i^f . At $\tau = 0$ we have $g_1^f = -f$. As the filament folds g_1^f changes sign saturating to $g_1^f = f$. The time τ_0 at which $g_1^f(\tau_0) = 0$ can be designated as the folding time. We find this value of the folding time to depend on the initial configuration of the filament. The end of the filament at which the force is applied, moves by a distance $x_1(\tau)$ at time τ . This is depicted in figure 6 along with the length of the fold.

For $\tau \gg \tau_0$ all the distances scale as $\tau^{1/2}$. This shows that in this regime the problem is similar to that of stretching a tense string [22]. For large f we can then neglect the contribution from the curvature energy and noise. The dynamics is then determined by the straight segment up to the fold moving through the fluid. This results in a linear tension profile along the filament [22], with the tension falling to zero approximately at the fold.

At $s = 0$, $g^f(s = 0) = f$, by neglecting the curvature and noise terms on the right hand side of the equation 3, using dimensional analysis, we get, $x(s = 0, \tau) \sim (\tau)^{1/2}$. This is shown in figure 6.

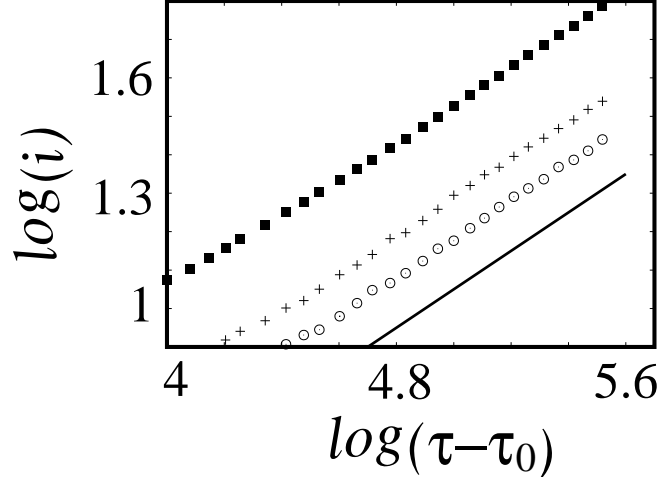


FIG. 6 The displacement of $x_1(\tau)$ after folding of the filament (Filled squares). Crosses shows the position of the fold along the contour. Open circles represent the arc length up to which g^f is linear. $(\tau - \tau_0)^{1/2}$ line (solid line) is given as a guide to the eye

As the end moves, the position of the fold moves along the contour (see figure 1). Hence the fold length and the point at which tension falls to zero too follow similar behavior as that of $x(s = 0, \tau)$.

To conclude, we have studied the dynamics of a single semiflexible filament under the action of a compressing force at one end which lead to folding. We have shown that the folding length(l_f) of the filament is proportional to $\sqrt{\kappa}$ and decreases monotonically with the applied force f . This follows from the fact that the tension in semiflexible filaments decay exponentially along the contour. It is shown that buckling of a homogeneous elastic rod with an exponential tension profile is qualitatively similar to that of the folding of a semiflexible filament. The folding length for a given κ and force \mathbf{f} does depend on the strength of the noise η . Thus once the initial configuration is chosen, a "zero temperature" calculation should give the same results. As the filament folds the tension changes sign and

we move into the stretching regime. We have shown, using numerical simulations and scaling arguments, that in this regime the fold length, the end point $x_1(\tau)$ and the distance along the contour to which tension has propagated, scales as $\tau^{1/2}$.

Acknowledgments

We would like to thank S. K. Srivatsa and Madan Rao for many discussions and comments. P.B.S. thanks U. Seifert for discussions during a stay at MPIKG, Golm. We thank CSIR, India for financial support.

REFERENCES

- [1] T. R. Strick *et al.*, *Science*, **271**, 1835 (1996)
- [2] A. Ashkin, *Science*, **210**, 1081 (1980)
- [3] M. Dogterom and B. Yurke, *Science* **278**, 856 (1997)
- [4] M. S. V. Kellermayer *et al.*, *Science* **276**, 1112 (1997); L. Tskhovrebova, *et al.*, *Nature*, **387**, 308 (1997)
- [5] S. B. Smith, Y. Cui, and C. Bustamante, *Science* **271**, 795 (1996); P. Cluzel *et al.*, *Science* **271**, 792 (1996)
- [6] A.C. Maggs, *Phys. Rev. E.*, **55**, 7396 (1996).
- [7] E. Frey, *Advances in Solid State Physics*, **41**, 345 (2001).
- [8] See, e.g., B. Alberts *et al.*, *Molecular Biology of the Cell* (Garland Publ., New York, 1983).
- [9] P. A. Janmey *Curr. Op. Cell. Biol.*, **2**, 4 (1991), *Hand book of Biological Physics, Chapter 17, Page 805*, North Holland, Amsterdam (1995)
- [10] F. Gittes *et al.*, *J. Cell. Biol.*, **120**, 923 (1993)
- [11] A. Ott, M. Magnasco, A. Simon, and A. Libchaber, *Phys. Rev. E* **48**, R 1642 (1993)
- [12] L. D. Landau and E. M. Lifshitz *Theory of Elasticity* (Pergamon, Oxford, 1986)
- [13] L. Golubović, D. Moldovan and A. Peredera, *Phys. rev. Lett.* **81**, 3387 (1998)
- [14] F. Gittes *et al.*, *Biophys. J.* **70**, 418 (1996)
- [15] T. Odijk *J. Chem. Phys.*, **108**, 6923 (1998)
- [16] P. Ranjith and P. B. Sunil Kumar, *to be published*
- [17] E. Frey, K. Kroy, J. Wilhelm and E. Sackmann. *Dynamical Networks in Physics and*

Biology, edited by D. Beysens and G. Forgacs (EDP Sciences - Springer, Berlin, 1998).

[18] M. D. Wang *et al*, *Biophys. J.*, **72**, 1335 (1997)

[19] D. Bensimon, D. Dohmi, M. Mézard *Europhys. Lett.*, **42**(1), 97-102 (1998)

[20] P. Grassia and E. J. Hinch, *J. Fluid Mech.* **308**, 255 (1996)

[21] M. Doi and S.F Edwards, *The Theory of Polymer Dynamics* (Clarendon Press, Oxford, 1986)

[22] U. Seifert, W. Wintz, and P. Nelson, *Phys.Rev.Lett.* **77**,5389 (1996).